Supplementary Materials

FIG. S1. Enrichment of shRNA clones, Flow cytometry based image stream and immune-blot analysis showing re-activation of latent HIV-1 provirus in Jurkat T-cell line 2D10 is independent of canonical NF-κB signaling cascade.

FIG. S2. Reactivation of latent HIV-1 proviruses by ESR-1 and NCOA1 antagonists.

FIG S3. ESR1-interacting and estrogen-related pathway proteins are enriched in the shRNA screen.

FIG. S4. Cell activation state of quiescent Th17 cells before and after TCR stimulation.

FIG. S5. Effect of β-estradiol and SERMs on HIV-1 reactivation in the QUECEL (Th17) primary cell model of HIV-1 latency.

FIG. S6. β-estradiol concentrations in serum and media and expression levels of ESR1 in primary CD4 T cells in a male and female donor.

FIG. S7. Limiting dilution assay comparing values obtained by the EDITS assay and the maximum likelihood method and correlation between model systems and patient samples.

FIG S8. ESR agonists inhibit latency reversal, while ESR antagonist induce latency reversal, ex vivo.

FIG. S9. Tamoxifen and related SERMs synergize with SAHA to promote HIV-1 reactivation in female patients.

Fig. S10. Effect of ESR agonists and antagonists on post-menopausal women.

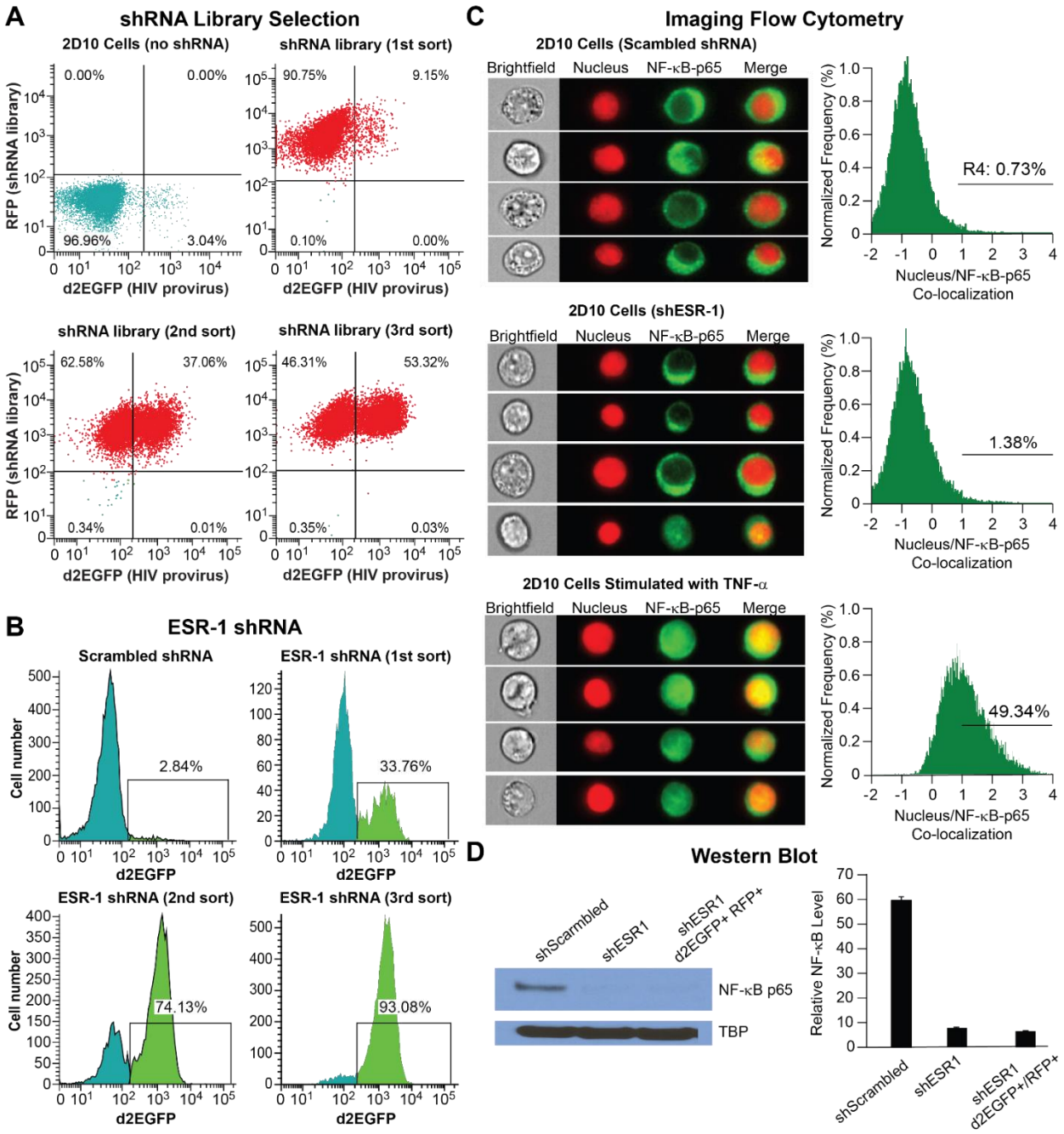

FIG. S1. Enrichment of shRNA clonesand flow cytometry based image stream and immune-blot analysis showing re-activation of latent HIV-1 provirus in Jurkat T-cell line 2D10 is independent of canonical NF-κB signaling cascade. **(A)** Sequential flow cytometry based sorting of GFP+, RFP+ cells representing shRNA infected constitutively re-activated population, enriching the clonal population. **(B)** Enrichment of ESR-1 specific shRNA knock-down cells by sequential flow cytometry based sorting enrichening constitutively re-activated population. Cells infected with lentiviral vector expressing scrambled shRNA and selected in puromycin. Middle: 2D10 cells with infected with shESR1 lentiviral vector. The ESR-1 mRNA target specific sequence was taken from the shRNA library database provided by Cellecta Inc. (Mountainview, CA) human ESR-1 shRNA was obtained from GE Dharmacon:

5'-CTACAGGCCAAATTTAGATAAGTTAATATTCATAGCTTATCTGAATTTGGCCTGTAG-3'

VSV-g pseudotyped single round virus was produced by co-transfection of Lenti shESR-1 shRNA, pCMVdR8.91r and pCMV-VSV-g in HEK 293T cells using lipofectamine 2000. Latently infected 2D10 cells (106 per ml) were superinfected with an m.o.i. of 1.8. shRNA infected cells and selected in puromycin media. **(C)** Image stream analysis of nuclear localization of NF-κB-p65 in 2D10 cells. Note that ESR1 knockdown did not result in nuclear import of NF-κB-p65 com as also evident in scrambled control [Top and Middle]. Nuclear localization of NF-κB-p65 in 2D10 cells after TNF-α (6 ng/ml) stimulation [Bottom]. **(D)** Immuno blot analysis of nuclear extracts showing nuclear NF-κB-p65 in ESR1 knock-down (KD) cells compared to cells with scrambled shRNA Left: Immuno-blot for NF-κB-p65 (top). TATA binding protein (TBP) was used as internal loading control (bottom).. Right: Densitometry analysis (Image J analysis) of three independent immune-blot analysis with nuclear extracts showing significantly low level of NF-κB-p65 compared to cells with scrambled shRNA.

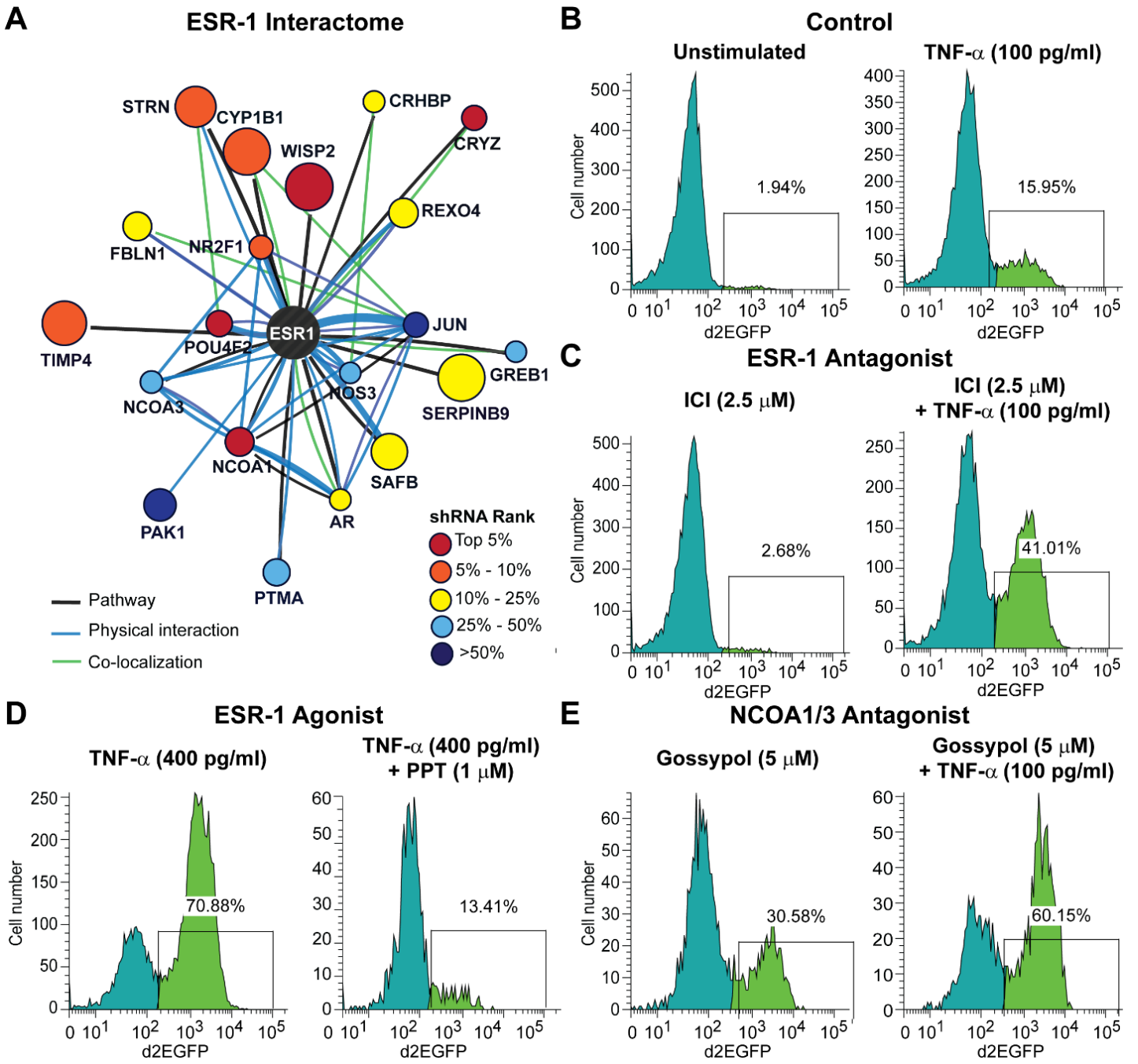

FIG. S2. Reactivation of latent HIV-1 proviruses by ESR-1 and NCOA1 antagonists. (**A**) GENEmania analysis for ESR-1 and its interacting molecules. The shRNA targets obtained from the shRNA library screening were ranked as per the abundance values. Top 10% hits were used as input molecules to perform Ingenuity Pathway AnalysisTM (IPA) to generate a functional network based on the information contained in the Ingenuity Pathways Knowledge Base. Networks of those focus genes, along with other related genes/molecules generated by the Knowledge Base, and were then algorithmically generated based on their connectivity (1). In addition, a web-based tool, GeneMANIA, was used to generate highly accurate prediction algorithm to construct a network using ESR-1 as query (2). The default advanced settings were used for GeneMANIA analysis for pathway, physical interactions, and co-localization to build a network model. Query-dependent network weighting was set as the automatically selected weighting method that identified the top related genes. The molecules in the GeneMANIA network were then compared with shRNA library screening data to identify the abundance-based rank of each of the potential ESR-1 related molecules. The ranking of hits found in the network is indicated by the color coding. Note that the ESR-1 costimulatory molecule, nuclear receptor co-activator 3 (NCOA3), is also a high ranking hit in the shRNA screen. (**B**) Control 2D10 cells showing basal d2GFP+ expression levels (left) and partial reactivation by 100 pg/ml TNF-α. (**C**) Reactivation of 2D10 cells by the ESR-1 antagonist Fulvestrant (ICI-182780, 2.5 μM). in the absence (left) or presence of 100 pg/ml TNF-α. (**D**) Inhibition of TNF-α by the ESR-1 agonist 4,4’,4”-(4-Propyl-[1H-pyrazole-1,3,5-triyl) trisphenol (PPT) (right). Cells reactivated by 400 pg/ml TNF-α in the absence of PPT (left). (**E**) Reactivation of latent HIV-1 by the NCOA1/3 agonist, gossypol (5 μM) in the absence (left) or presence (right) of 100 pg/ml TNF-α.

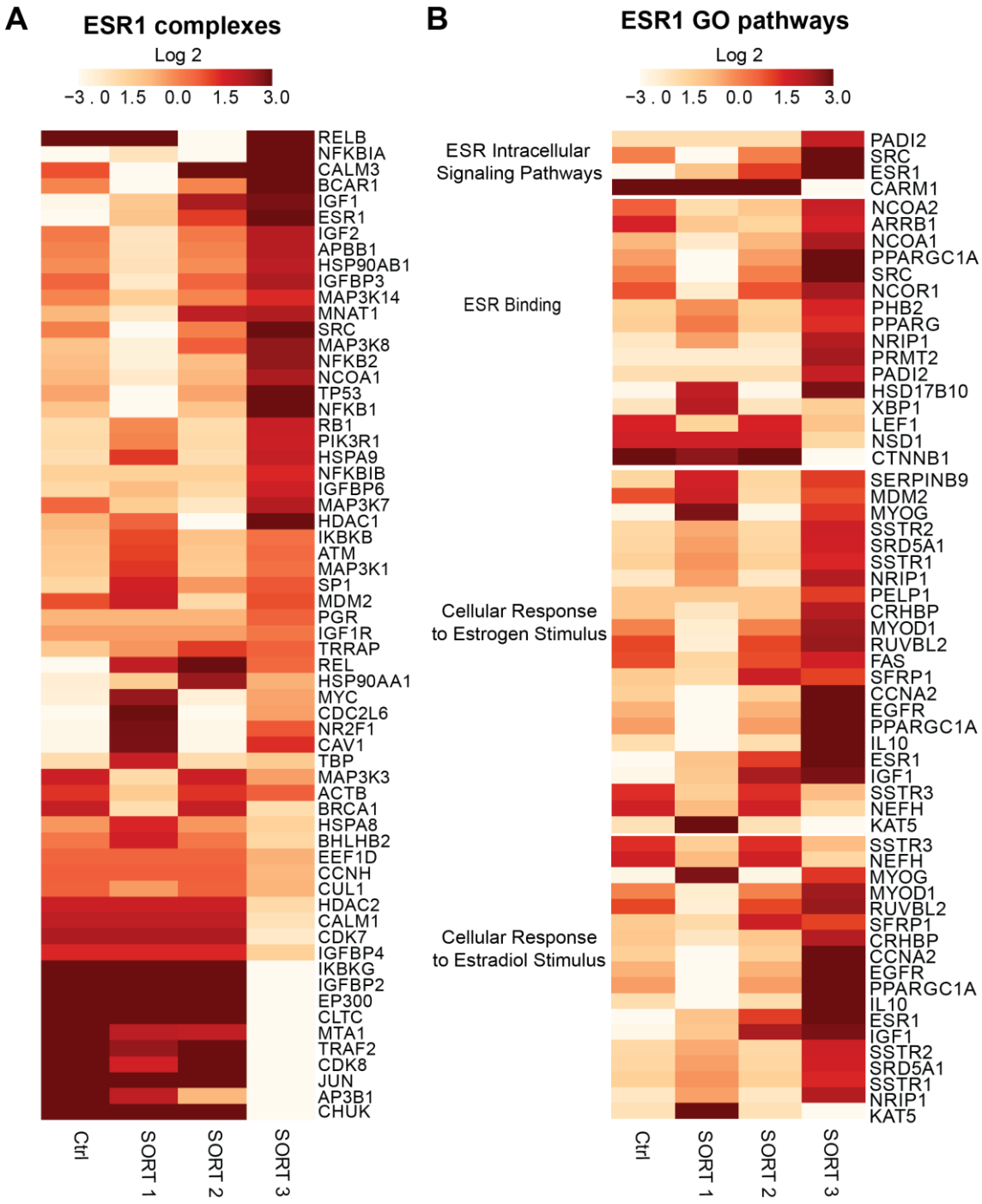

FIG S3. ESR1-interacting and estrogen-related pathway proteins are enriched in the shRNA screen. (A) ESR1-containing human complexes from the CORUM and PCDq databases were used to identify ESR1-interacting factors. Log2 enrichment values for the pooled ESR1-interacting proteins were derived from shRNA repressor screen sorts 1 through 3 (module 1) and used to generate the heat map, with the values from the activator screen plotted as control. (B) The Gene Ontology (GO) terms were used to identify genes related to estrogen response and signaling pathways. The enrichment level of the genes listed in each GO term that were represented in the Cellecta shRNA library was used to plot the heatmap as described for A. Analysis of the shRNA repressor screen data was performed using edgeR as described (3). Briefly, read counts per shRNA clone were filtered by removal of those with a count value less than 5 CPM. Multidimensional scaling plots were used to confirm the consistency between replicate samples. To determine the level of differential enrichment, the level of representation of genes in the repressor screen samples was compared to that of samples from the activator screen treated under similar conditions using generalized linear models. The results from all shRNAs targeting the same gene were summarized to obtain gene-level enrichment data per replicate group. p-values and FDRs were calculated from the enrichment values obtained from the repressor-activator screen comparison. To combine results between different non-replicate samples, the geometric mean of the log2-transformed enrichment levels was obtained and the FDR values were combined using Fisher's method. Genes were ranked based on their average level of enrichment in samples corresponding to sorts 2 and 3.

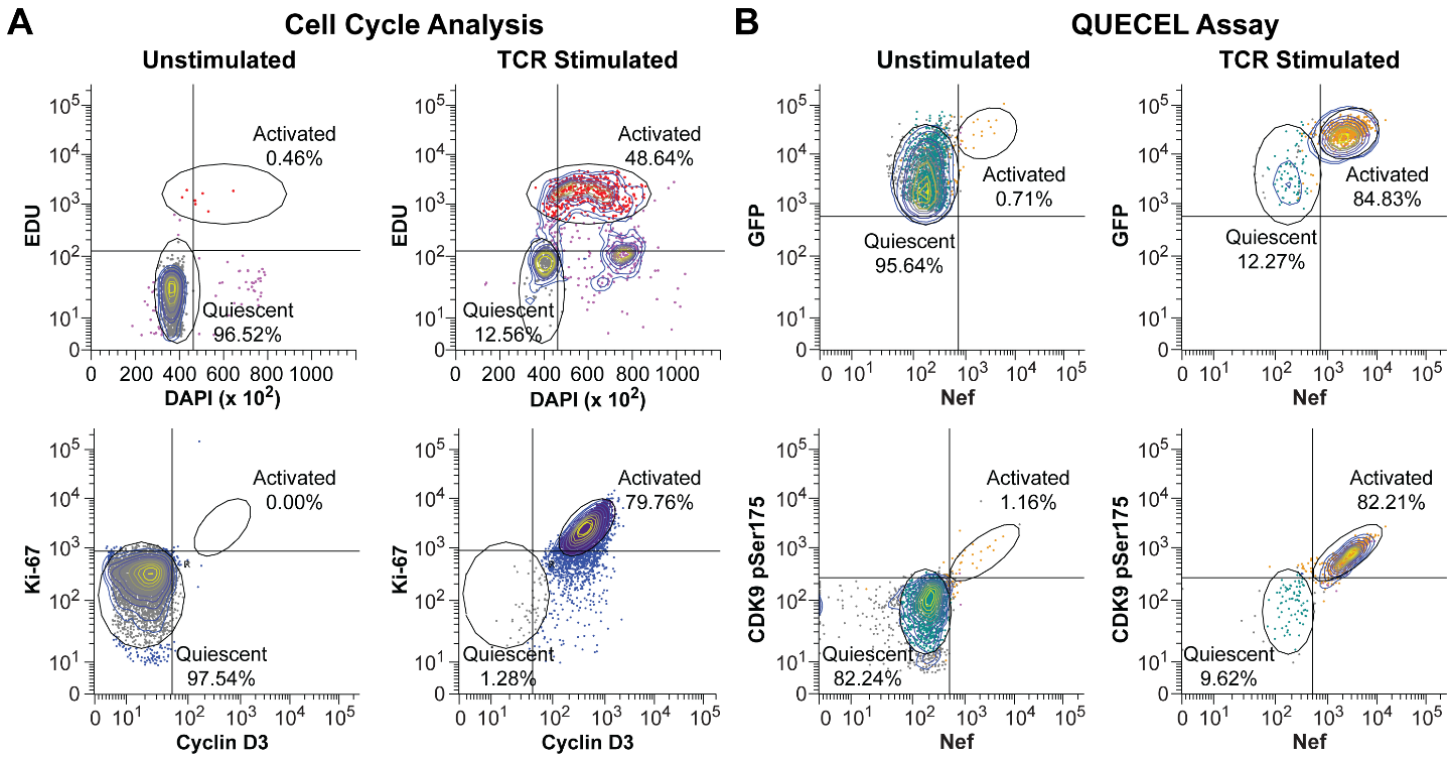

FIG. S4. Cell activation state of quiescent Th17 cells before and after TCR stimulation. (**A**) Cell cycle analysis. Cells were assayed at day 21 of the QUECEL (Th17) protocol. Quiescent Th17 Cells enter into cell cycle after 16 hr stimulation through the T cell receptor. Top panels: vertical axes represents DNA EDU incorporation and the horizontal axes represents total DNA as measured by DAPI fluorescence. Cells in S phase are positive for EdU and have a broad distribution of DNA content. Cells in G_0 show no EdU incorporation and have a diploid DNA content (left). Cells in G1 and G2/M2 have somewhat increased EdU incorporation and have either diploid of tetraploid DNA contents (right). Bottom panels: vertical axes represent Ki-67 expression, a marker of cellular proliferation, while the horizontal axes represents Cyclin D3 expression, which is required for a cell to leave G_0 phase. (**B**) QUECEL Assay.

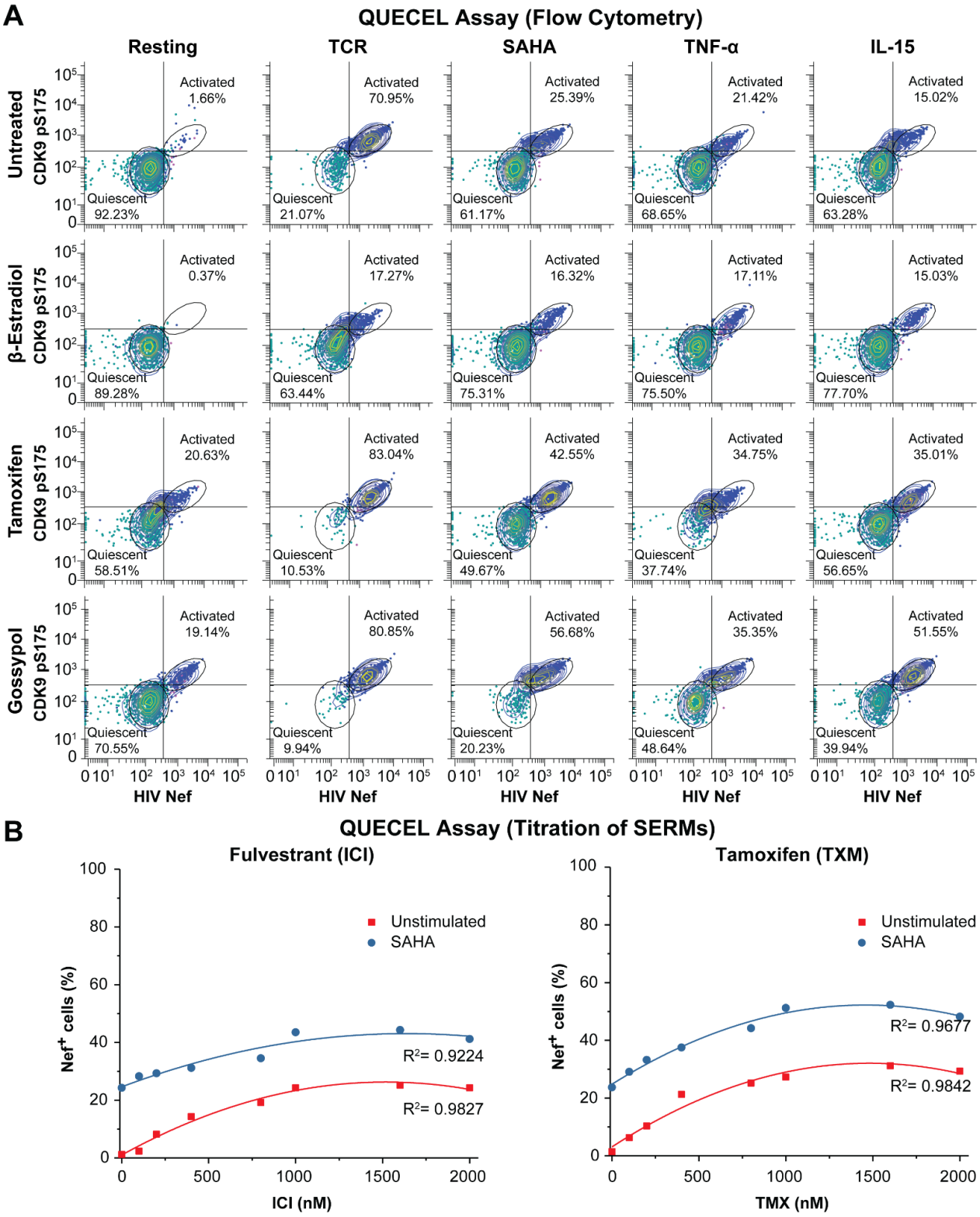

FIG. S5. Effect of β-estradiol and SERMs on HIV-1 reactivation in the QUECEL (Th17) primary cell model of HIV-1 latency. (**A**) Flow cytometry: the vertical axis measures intracellular levels of the phosphorylated P-TEFb subunit pSer175 CDK9, a marker of cellular activation, while the horizontal axis measures HIV-1 Nef, a maker of proviral transcription. Activated cells are present in the upper right hand quadrant as indicated by the circular gate. The flow plots are a representative subset of the data presented in **FIG 2**. Cells were pretreated with 300 pg/ml β-estradiol, 1 μM Gossypol, or 1 μM Tamoxifen for 2 hrs and then activated through TCR stimulation (Dynabeads® Human T-Activator CD3/CD28; 25 μl/10^6 cells), SAHA (500 nM), TNF-α (10 ng/ml) or IL-15 (10 ng/ml). Note that β-estradiol prevented >80% of the cells from responding to TCR stimulation. Tamoxifen partially activated HIV-1 and showed additive effects when combined with SAHA or IL-15. **(B)** Titration of Fulvestrant (ICI) and Tamoxifen (TXM) using the Th17 model of HIV-1 latency. Left: ICI titration with or without 500 nM SAHA. Right: TXM titration with or without 500 nM SAHA.

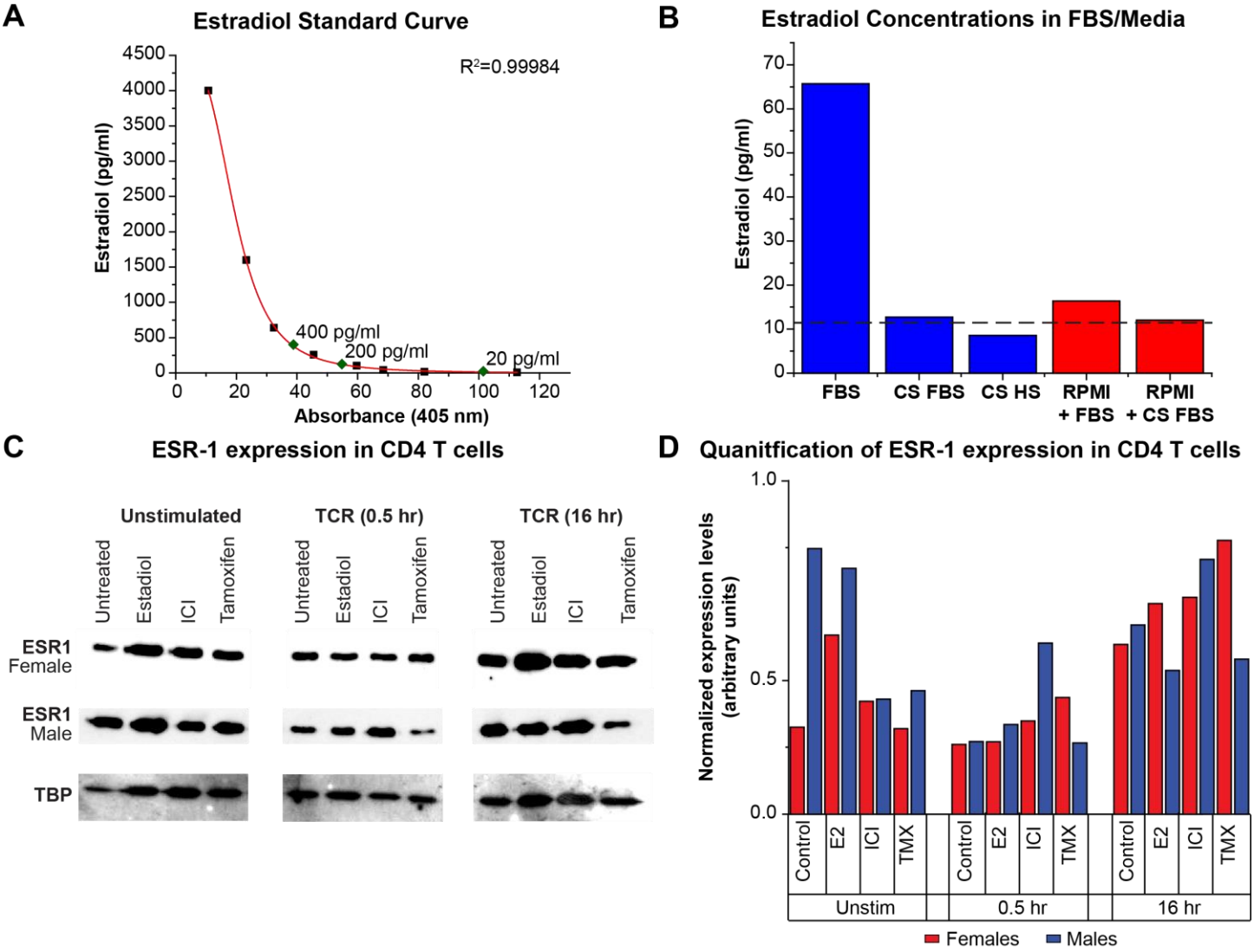

FIG. S6. β-estradiol concentrations in serum and media and expression levels of ESR1 in primary CD4 T cells in a male and female donor. (**A**) β-estradiol levels were measured by ELISAs. Standard curve of β-estradiol concentrations. Green points represent β-estradiol concentrations from stock solutions diluted for use in the experiments. (**B**) Concentration of β-estradiol in fetal bovine serum (FBS), charcoal stripped fetal bovine serum (CS FBS) and charcoal stripped human serum (CS HS) and RPMI with serums (red bars). The limit of detection in the assay is approximately 10 pg, as indicated by the dotted line. (**C**) Western blots of ESR1 expression in resting CD4 T cells. Total CD4 T cells were isolated from one male and one female donor. They were treated with nothing, Estradiol (300pg/ml), ICI (1uM) or Tamoxifen (1uM) for two hours prior to TCR stimulation using Dynal beads. After either 30 minutes of 16 hrs of stimulation, cells were collected and nuclear extracts were collected. TATA binding protein (TBP) was used as a loading control. **(D)** Quantification of the western blot using Image J software. Values are arbitrary units normalized to TBP expression levels.

A

Limiting Dilution Assay (Mapped Reads)

Male SF2511

1.00E+03	1.00E+04	1.00E+05	1.00E+06
568	456	5259	55789
659	2456	5347	52118
456	563	5572	48105
4694	2455	4621	50075
659	145	6656	51282
547	548	5408	54566
413	456	7868	48830
785	2833	5907	51582

Maximum Likelihood estimate: 58.24
95% Confidence Interval: {23.63, 143.53}

Female SF2457

1.00E+03	1.00E+04	1.00E+05	1.00E+06
648	369	4943	56071
529	1865	5628	58189
565	5656	5136	56603
645	696	5162	55076
563	565	5550	55248
544	2364	6057	52054
636	2463	6016	47652
2375	659	5615	60164

Maximum Likelihood estimate: 58.24
95% Confidence Interval: {23.64, 143.53}

Male SF2239

1.00E+03	1.00E+04	1.00E+05	1.00E+06
432	3432	8853	85345
543	2342	7894	79403
542	543	7313	85493
432	5432	7643	79583
452	3423	8593	89453
564	652	6423	74234
4534	234	8435	89482
675	5422	8453	79034

Maximum Likelihood estimate: 103.01
95% Confidence Interval: {45.02, 235.68}

B

RNA+ Cells per 10^6 (Background Subtracted)

Male SF2511

1.00E+03	1.00E+04	1.00E+05	1.00E+06
0.26	0.21	6.09	59.24
0.31	1.14	6.20	55.71
0.21	0.26	6.45	51.79
2.17	1.14	5.36	53.72
0.31	0.07	7.70	54.89
0.25	0.25	6.27	58.06
0.19	0.21	9.08	52.50
0.36	1.16	6.84	55.19

EDITS value: 55.14 +/- 2.40
95% Confidence Interval: {52.74, 57.54}

Female SF2457

1.00E+03	1.00E+04	1.00E+05	1.00E+06
0.30	0.17	5.73	59.50
0.25	0.87	6.52	61.52
0.26	2.62	5.95	60.01
0.30	0.32	5.98	58.55
0.26	0.26	6.43	58.72
0.25	1.10	7.01	55.64
0.30	1.14	6.96	51.34
1.10	0.31	6.50	63.37

EDITS value: 58.58 +/- 3.46
95% Confidence Interval: {55.12, 62.04}

Male SF2239

1.00E+03	1.00E+04	1.00E+05	1.00E+06
0.20	1.59	10.20	85.77
0.25	1.09	9.11	80.70
0.25	0.25	8.45	85.89
0.20	2.51	8.82	80.86
0.21	1.59	9.90	89.19
0.26	0.30	7.43	76.19
2.10	0.11	9.72	89.22
0.31	2.52	9.74	80.39

EDITS value: 83.52 +/- 4.39
95% Confidence Interval: {79.13, 87.91}

< 2000 < 1.0

Cut off values

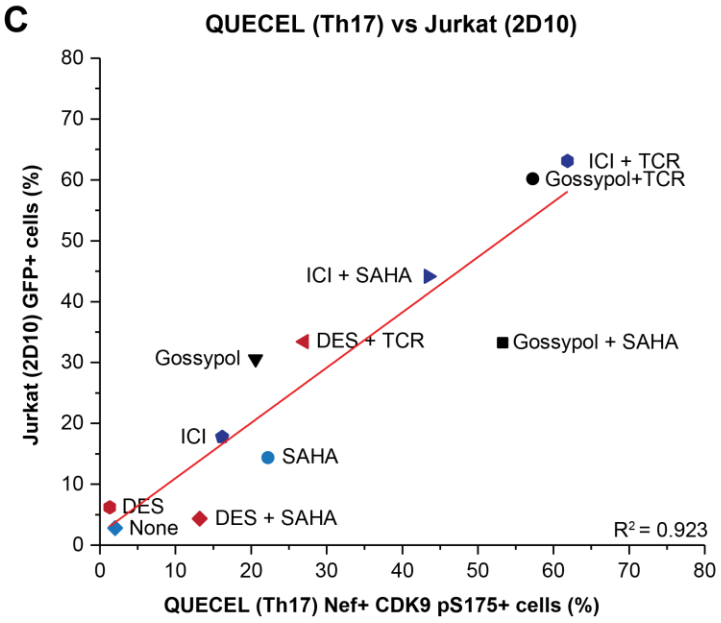

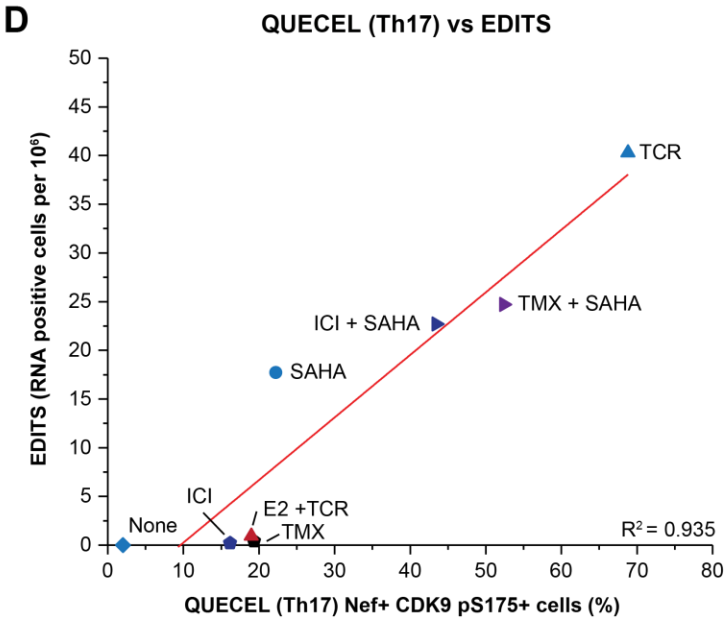

FIG. S7. Limiting dilution assay comparing values obtained by the EDITS assay and the maximum likelihood method and correlation between model systems and patient samples. (**A**) Cells from three donors (Male SF2511, Female SF2457, Male SF2239) were plated in 96 well plates at concentrations of 10^3, 10^4, 10^5, and 10^6 cells per well in sets of 8 replicates each. EDITS assays were performed on each well and the reservoir size was estimated either by the maximum likelihood method (4). (**B**) EDITS analysis of induced cell numbers obtained by averaging each of the EDITS values for the well containing 10^6 cells per well. The data is the same as in Panel A. Note that the two methods give approximately the same estimates, but the EDITS values have much higher confidence limits. (**C**) QUECEL (Th17 cell) primary cell model compared to 2D10 Jurkat model.assay of latency reversing agents. Cells were pretreated with SERMs, Estradiol or nothing for 2 hrs then stimulated with multiple LRAs for 16 hrs. The vertical axis shows GFP expression in 2D10 Jurkat T cells while horizonal axis shows Nef and CDK9 pS175 double positive cells. R^2= 0.923 and n=11. **(D)** Th17 primary cell model compared to EDITS patient samples. The vertical axis shows the number of cells with a positive EDITS signal and the horizonal and the horizonal axis shows Nef and CDK9 pS175 double positive cells. R^2= 0.935 and n= 8.

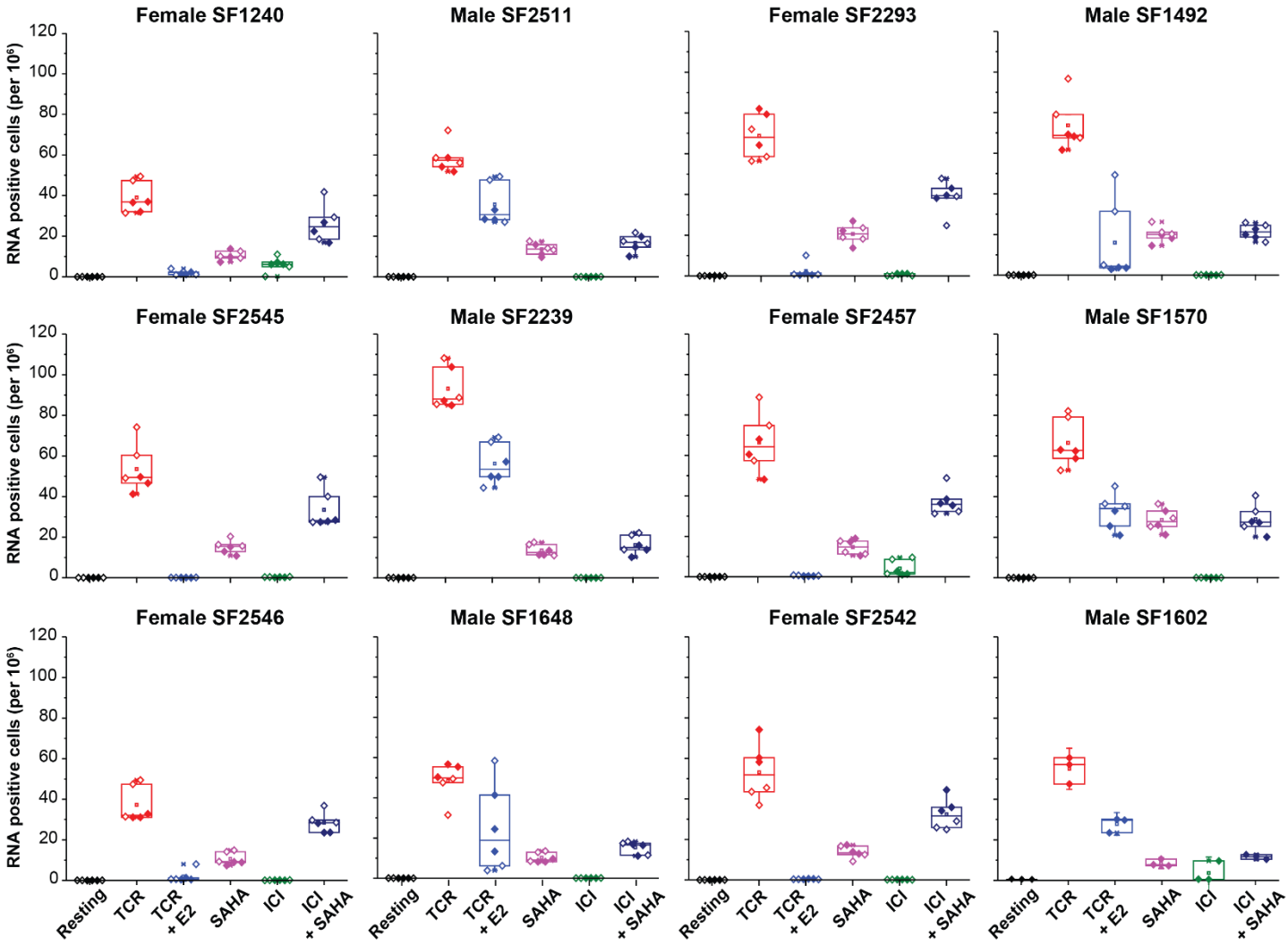

FIG S8. ESR agonists inhibit latency reversal, while ESR antagonist induce latency reversal, ex vivo. *Ex vivo* induction of HIV-1 transcription in leukapheresis samples from ART-treated women and men. Data are the individual samples described in FIG. 5. Solid circles: PGM. Open symbols: S5. For the S5 data the entire sample set, together with its standard curve, was run simultaneously on one 540 chip. Male SF1602 was assayed only using the S5 sequencer. To determine whether the difference in the size of reservoir between male and female donors was statistically significant, targeted RNA-seq data from six male and six female donors were obtained using two sequencing platforms (PGM and S5) with three replicates per condition. The replicates were performed on separate samples drawn from the frozen PBMCs in leukapheresis pool over a period of several months. The data were analyzed using linear mixed effects models suitable for analysis of RNA-seq-based data, with donors as random variables and sequencing platforms as blocking variables. The PGM samples were sequences in three separate runs with individual standard curves, while the S5 samples were run on the larger chip as a pool with a single standard curve. As expected, differences between the sequencing runs was the source of the largest variation demonstrating that blocking was warranted to remove this non-biological source of noise. Note that TCR stimulated reactivation is abrogated in the presence of β-estradiol in women. Conversely, treatment with Fulvestrant and SAHA enhanced the transcription to higher levels than seen with SAHA alone in women.

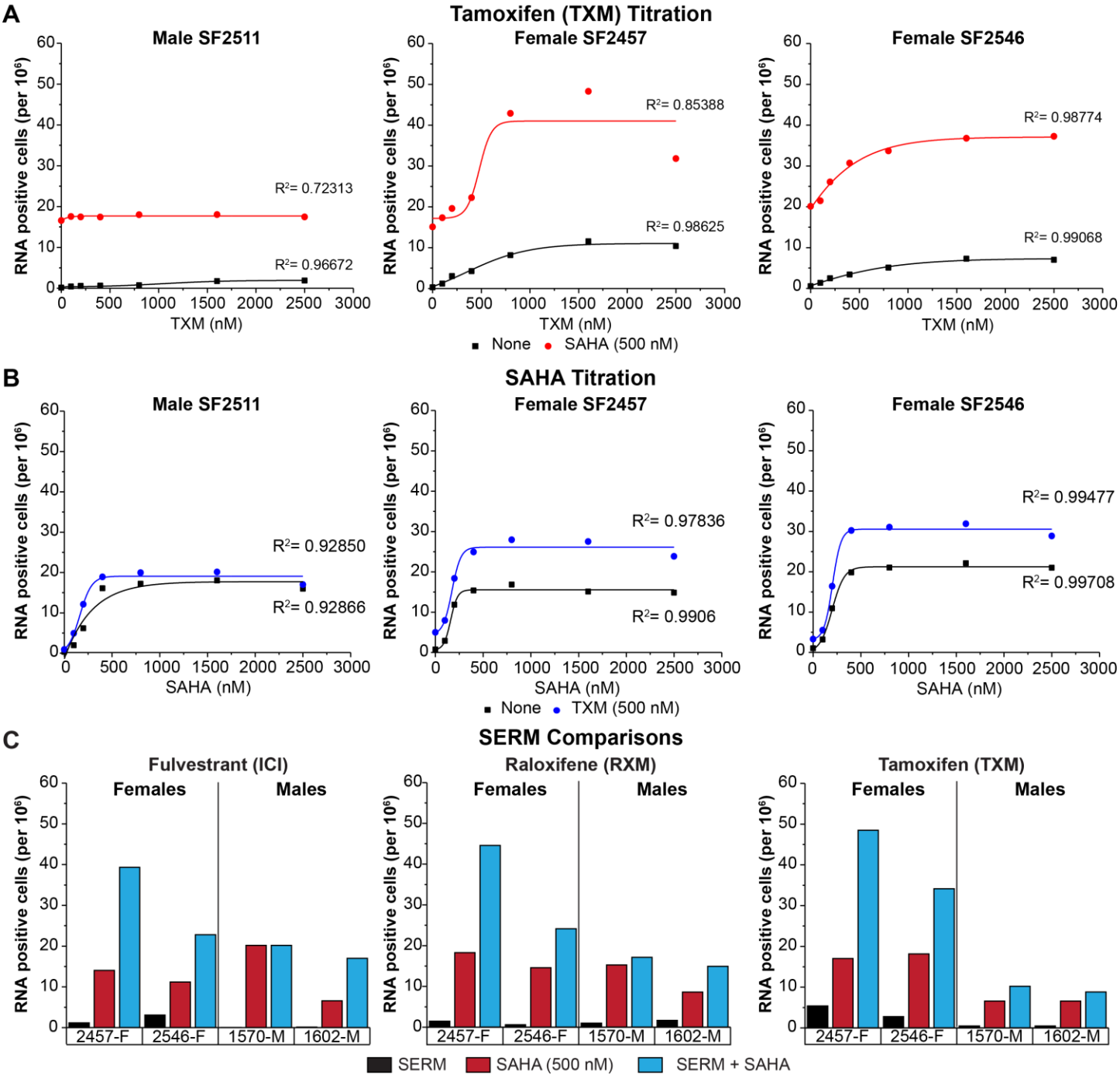

FIG. S9. Tamoxifen and related SERMs synergize with SAHA to promote HIV-1 reactivation in female patients. EDITS assays were performed to measure ex vivo induction of HIV-1 transcription as described in the legend to Fig. 7. (**A**) Tamoxifen titration in the presence of 500 μM SAHA using 1 male and 2 female donors. (**B**) Reciprocal titration of SAHA with Tamoxifen (500 nM). Note that the combination of Tamoxifen and SAHA has a synergistic effect on 2 female donors and little effect on the male donor. Curves are fit using a Boltzmann sigmoidal fit for both titrations. (**C**) EDITS assays were performed using four well-suppressed HARRT treated patients (two females (left) and two males (right). HIV-1 transcription was stimulated using either 1 μM SERM, 500 nM SAHA or a combination of SERM and SAHA. For each SERM (Fulvestrant 1 μM, Raloxifene, 1 μM, Tamoxifen (1 μM), SAHA has an additive or synergistic effect on the reactivation of HIV-1 transcription. This occurs in both males and females, however synergism is only seen in females.

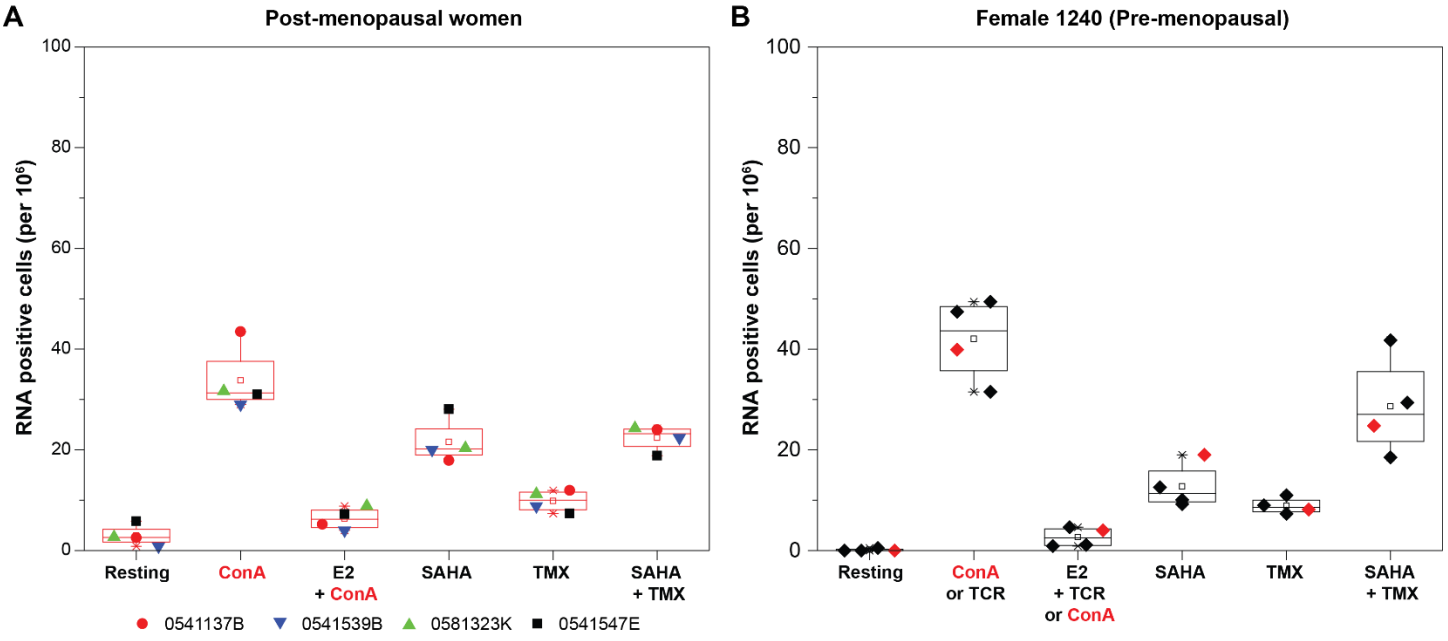

Fig. S10. Effect of ESR agonists and antagonists on post-menopausal women. (**A**) EDITS assays were performed on four HAART treated post-menopausal women. Maximal T-cell activation was obtained in this experiment using 10 ng/ml ConA. β-estradiol strongly repressed HIV-1 transcription in the presence of ConA stimulation, similar to the effects seen in pre-menopausal women. Tamoxifen (1 μM) was a weak activator of HIV-1 transcription, as also seen in pre-menopausal women, but not in men. Treatment with 500 μM SAHA resulted in a stronger relative activation in this particular cohort compared to pre-menopausal women, and consequently additive effects between Tamoxifen and SAHA were not observed. (**B**) Control assays using patient SF1240. Black diamonds indicate prior data obtained using TCR instead of ConA as a stimulus. Red diamonds are data from the EDITS assay run simultaneously with the samples in Panel A. Note that maximal cell activation was achieved using either TCR or ConA as a stimulus. The strong inhibition by estradiol is evident in both sample sets.

References

1. Das B*, et al.* (2010) Influence of p53 in the transition of myotrophin-induced cardiac hypertrophy to heart failure. *Cardiovascular research* 87(3):524-534.
2. Yang C, Chen P, Zhang W, & Du H (2016) Bioinformatics-Driven New Immune Target Discovery in Disease. *Scandinavian journal of immunology* 84(2):130-136.
3. Dai Z*, et al.* (2014) edgeR: a versatile tool for the analysis of shRNA-seq and CRISPR-Cas9 genetic screens. *F1000Research* 3:95.
4. Rosenbloom DI*, et al.* (2015) Designing and Interpreting Limiting Dilution Assays: General Principles and Applications to the Latent Reservoir for Human Immunodeficiency Virus-1. *Open forum infectious diseases* 2(4):ofv123.